

Article

Bio-Lubricant Properties Analysis of Drilling an Innovative Design of Bioactive Kinetic Screw into Bone

Carlos Aurelio Andreucci ¹, Elza M. M. Fonseca ^{2,*} and Renato N. Jorge ³

¹ Mechanical Engineering Department, Faculty of Engineering, University of Porto, Rua Dr. Roberto Frias, 712, 4200-465 Porto, Portugal

² LAETA, INEGI, ISEP, Instituto Politécnico do Porto, R. Dr. António Bernardino de Almeida, 4249-015 Porto, Portugal

³ LAETA, INEGI, Mechanical Engineering Department, Faculty of Engineering, University of Porto, Rua Dr. Roberto Frias, 712, 4200-465 Porto, Portugal

* Correspondence: elz@isep.ipp.pt

Abstract: Biotribology is applied to study the friction, wear, and lubrication of biological systems or natural phenomena under relative motion in the human body. It is a multidisciplinary field and tribological processes impact all aspects of our daily life. Tribological processes may occur after the implantation of an artificial device in the human body with a wide variety of sliding and frictional interfaces. Blood is a natural bio-lubricant experiencing laminar flow at the lower screw velocities associated with drilling implants into bone, being a viscoelastic fluid with viscous and fluid characteristics. The viscosity comes from the blood plasma, while the elastic properties are from the deformation of red blood cells. In this study, drilling parameters according to material properties obtained by Finite Element Analysis are given. The influence of blood on the resulting friction between the surfaces is demonstrated and correlated with mechanical and biological consequences, identifying an innovative approach to obtaining a new lubricant parameter for bone drilling analysis. The lubrication parameter (HN) found within the limitations of conditions used in this study is 10.7×10^{-7} for both cortical bone (D1) and spongy bone (D4). A thermal-structural analysis of the densities of the soft bone (D4) and hard bone (D1) shows differences in only the equivalent stress values due to the differences in respective Young moduli. The natural occurrences of blood as a lubricant in bone-screw perforations are poorly investigated in the literature and its effects are fundamental in osseointegration. This work aims to elucidate the relevance of the study of blood as a lubricant in drilling and screwing implants into bone at lower speeds.

Keywords: bio-lubricant; lubrication parameter; bone drilling; blood; bioactive kinetic screw



Citation: Andreucci, C.A.; Fonseca, E.M.M.; Jorge, R.N. Bio-Lubricant Properties Analysis of Drilling an Innovative Design of Bioactive Kinetic Screw into Bone. *Designs* **2023**, *7*, 21. <https://doi.org/10.3390/designs7010021>

Academic Editors: Richard Drevet and Hicham Benhayoune

Received: 18 December 2022

Revised: 18 January 2023

Accepted: 29 January 2023

Published: 1 February 2023



Copyright: © 2023 by the authors. Licensee MDPI, Basel, Switzerland. This article is an open access article distributed under the terms and conditions of the Creative Commons Attribution (CC BY) license (<https://creativecommons.org/licenses/by/4.0/>).

1. Introduction

Blood is a special type of fluid connective tissue derived from mesoderm and composed of plasma (55%) and cellular elements (45%), erythrocytes (red blood cells), leukocytes (white blood cells), and thrombocytes (platelets). Its color changes according to the gas it carries within its structure, being bright red when carrying oxygen, or dark purple when carrying carbon dioxide. It represents 8% of body mass, is slightly alkaline (pH = 7.35–7.45), has a temperature of 37 °C, a viscosity 3 to 4 times greater than that of water, and its average volume in the human body is five liters [1]. Blood transports hormones to organs and causes them to change their physiology, regulates the pH, restricts fluid loss during an injury, acts as a defense against pathogens and toxins, and regulates the body temperature [2]. Plasma is the pale-yellow-colored liquid component of blood that holds its cellular elements in suspension and is constituted of water (91.5%), proteins (7%), namely albumins, globulins, and fibrinogen, and other solutes (1.5%) electrolytic ions, gases, nutrients, and waste products [3]. The function of plasma is to absorb, transport, and release heat through water, maintain osmotic balance through albumins and provide body

defense through globulins, blood clotting through fibrinogen, and pH buffering through its electrolytic ions. Red blood cells are circular biconcave non-nucleated cells, measuring 7 to 8 μm in diameter and 2.5 μm in thickness with a life span of 120 days, presenting red color (hemoglobin pigment) [4]. Red blood cells transport oxygen (oxyhemoglobin) from lungs to tissues and carbon dioxide (deoxyhemoglobin) from tissues to lungs via the hemoglobin molecules (Hb) that represent 13 to 15 g per 100 mL of blood. Each molecule of Hb carries four molecules of oxygen [5].

When drilling into bone tissue cuts a blood vessel, the body starts the process to keep homeostasis through hemostasis, which begins with the vascular phase, in which the diameter of the blood vessels decreases, and endothelial cells (the inner layer of blood vessels) releasing chemical factors; next, in the platelet phase, a platelet plug forms and other chemicals are released (ADP, clotting factors); then coagulation or blood clotting occurs, where in addition to platelets, fibrinogen is converted to fibrin to form a net-like structure to form a clot; finally, fibrinolysis occurs, and, after the blood vessel is completely healed and new connective tissue has formed, the now unnecessary blood clot is removed [6].

Blood behaves as a non-Newtonian fluid and its viscosity varies with shear rate, decreasing at high shear rates (shear-thinning fluid) and vice versa. Blood viscosity also increases with increases in red cell aggregability, in coagulating blood, falls with the thrombus formation, while in non-coagulation blood, retains almost the same value, as shown by the activated clotting time and fibrinogen concentration tests. Blood viscosity is determined by plasma viscosity, hematocrit (red blood cell volume), and the mechanical properties of red blood cells, mainly erythrocyte deformability and erythrocyte aggregation [7]. The viscosity, equivalent to friction in fluids, of blood at 37 °C is normally 4×10^{-3} pascal-seconds [8]. The friction arising from bone-implant contact (BIC) during drilling converts kinetic energy into thermal energy. Between bone-implant surfaces, blood flows naturally after the surgical cutting of the bone blood vessels during drilling, and filling this gap with blood is desirable to obtain the initial phase of inflammation and subsequent osseointegration. Hydrophilic features are desired on implant surfaces to attract and adhere blood in the initial process of inflammation in the bone-implant contact healing process [9]. Although surgery damages bone tissue, it also triggers a cascade of wound-healing events that stimulate osseointegration, improving implant stability through bone remodeling [10]. The shear rate (τ_{yx}) for a fluid flowing (blood) [11] between bone and a BKS implant, one moving at a constant speed (BKS) and the other stationary (bone) is determined by the change in pressure (ΔP), the distance between fluid flow (L) and the diameter of the bone-implant interface micro gap (y), defined by Equation (1):

$$\tau_{yx} = \frac{\Delta P y}{L} \quad (1)$$

The Stribeck curve is a fundamental concept in the field of tribology. It shows that friction in fluid-lubricated contacts is a non-linear function of the contact load, the lubricant viscosity, and the lubricant entrainment speed (sliding speed), differentiating boundary lubrication (bone-implant contact), mixed lubrication (bone-implant contact gap filled by blood) and hydrodynamic lubrication (load supported by hydrodynamic pressure) [12]. For the contact between two fluid-lubricated surfaces, the Stribeck curve shows the relationship between the so-called Hersey Number (HN) [13], a dimensionless lubrication parameter that shows the relationship between viscosity and load, and how friction changes with increasing velocity. The Hersey number is defined as Equation (2):

$$HN = \frac{\eta N}{P} \quad (2)$$

where η is the dynamic viscosity ($\text{Pa}\cdot\text{s} = \text{N}\cdot\text{s}/\text{m}^2$) of the fluid, N is the entrainment speed of the fluid, which is equal to the velocity of BKS Implant insertion (m/s), and P is the Insertion Torque applied (Nm).

Boundary lubrication is related to bone-implant contact without the effect of the blood as a lubricant and is commonly analyzed by insertion torque forces [13]. Hydrodynamic lubrication is related to the pressure in the plasma and cells involved in the inflammation process initiated by the surgical cut made by drilling into the bone. Mixed lubrication, the objective of this study, correlates the influence of roughness contact between the bone-implant load, supported by both surfaces and the liquid lubricant (blood) [13]. The mixed lubrication regime can be determined by the (λ) ratio of the film thickness to the root-mean-square (RMS) surface roughness of the two frictional surfaces. When $1 < \lambda < 3$ the lubrication condition is considered mixed lubrication. The RMS surface roughness of Ti6Al4V implants is in the range of 6–14 μm [14–16] depending on the surface treatment applied, and the roughness—the linear dimensions of the bone tissue—range from 5.5 to 6.5 μm , depending on the quality of the bone drilling cut [17]. Both can change either slightly or significantly during drilling wear. To maintain full blood film lubrication, the minimum film thickness must be greater than 15–18 μm , which is generally the case in actual physiological conditions when 150 μm is the distance between the screwed implant and the bone bed site after healing [18]. The analysis of the Stribeck curve shows that the lubricant decreases the coefficient of friction proportionally to the velocity applied, likewise when the lubricant is blood, higher speeds can also aggregate the red blood cells increasing its viscosity and decreasing its lubricant properties. Understanding the ideal speed for insertion torque in bone screw implants can optimize the use of the blood as a lubricant, inherent to the surgical cut of the drilling process, and maintain its biological properties, improving the healing process and predictable results in osseointegration [19].

The mechanical properties of bone tissue are widely studied and discussed in the literature [20]. Several properties can be quantified, including the stiffness (S), the ultimate load that corresponds to the load at failure, the energy or work to failure (U), and ultimate displacement. The elastic region, before yield, represents Young's modulus (material stiffness), and the plastic region, a post-yield nonlinear region that contains the ultimate stress and the failure point. Yield stress is the transition to nonlinear behavior, which means that the stress begins to cause permanent damage to the bone structure. The maximum stress and strain that the bone can sustain are called the ultimate stress (strength) and ultimate strain. These properties are strongly dependent on the loading mode (tensile, compression, bending, or shear) and determine the mechanical response of the bone tissue to drilling operations [21]. Bone density varies between individuals and throughout life. A basic concept accepted in the literature is the structural and functional properties differences between cortical bone and trabecular bone. Trabecular bone has the same structures as compact bone, but they are not arranged in osteons, containing the same components. Instead, it has very distinct trabeculae (small beams of bone) separated by macroscopic spaces filled with red bone marrow or yellow bone marrow. The trabeculae are organized on the long lines of stress and help to reduce the weight of the bone [22]. The less-dense trabecular bone presents larger spaces (lacunae) in its composition, filled with higher blood quantity than cortical bone [23]. Maximum insertion Torque analyses clearly show the influence of different bone densities, and their relationship is robustly described in the literature. However, the lubricating effect of the blood into the bone-implant contact during drilling and screwing, and the lower torque obtained in the insertion of implants into trabecular bone, are not correlated in the literature and may influence these results [21].

The friction coefficient is independent of the applied normal force and displacement rate [24] but depends on the properties of the bone tissue surrounding the implant and on the properties of the implant surface [10]. The test of bone against implant surfaces produced a variety of different force-displacement curves and a wide range of friction coefficients (in the range of 0.19 to 0.78) [25–27].

Maximum insertion torque (MIT) values can range from 15 to 150 Ncm [28] with a mean value of 78.30 Ncm. The mean MIT is typically higher in D1 cortical bone (126.67 Ncm) and lower in D4 spongy bone (40.22 Ncm) [29]. A statistically significant correlation is found between bone volume and MIT values ($r = +0.771$, $p < 0.0001$). No sta-

tistically significant correlation is found between implant length and/or diameter and MIT in all bone densities. About 50–80% of bone-implant contact is described in the literature as clinically successful implants. Some results suggest that no matter the initial percentage of BIC, the final Osseointegration is about 58–60% BIC if the bone remodeling equilibrium state is reached [18].

Many studies on BIC are on the secondary stability (biological) of bone implants, and only the values of maximum insertion torque are described in primary or mechanical stability analysis, without the determination of BIC in this initial and fundamental phase to promote healing. Understanding BIC in primary stability, mainly in cases of high (D1) and low (D4) bone density increases our understanding of osseointegration. The interface between the implant and bone tissue presents a dynamic environment expressed by mechanical and biological interactions between the surfaces. The surgical trauma caused by drilling and screwing the screw into the bone promotes hemorrhage, the first and most important step of the healing process in osseointegration [3–7,14–16]. The objective of this work is to use finite element analysis (FEA) of drilling an implant into the bone with specific parameters to introduce innovative theoretical hypotheses of the correlation between blood as a natural biological lubricant, bone densities, maximum insertion torque, and a coefficient of friction that is a result of those interactions. The focus is on mechanical stability or primary stability and its immediate mechanical behaviors after bone plastic and elastic deformation due to the drilling and screwing process. Within the limitations of this study, we found a new lubrication parameter for bone drilling.

2. Materials and Methods

BKS is an innovative mechanical device with inherent biomechanical properties [22] including the bone compacting factor inside the BKS, allowing us to determine the absolute bone density through invasive direct measurement in the region of interest.

Applying simple biomechanical concepts of bone drilling, screwing, biocompatibility, and bone implant, the engineering design of BKS was created to, among other characteristics, optimize the surgical technique and reduce the trauma of bone perforation, with a smaller number of drillings, as seen in Figure 1.



Figure 1. BKS as a dental implant applied in the Finite Element Analysis drilling and screwing into the bone simultaneously.

In this work, three-dimensional finite element modeling and numerical analysis were carried out to facilitate thermal-structural analysis. The 3D models were built in Solidworks[®] and ANSYS 2020 R2[®]—Workbench 2020 R2 software programs. The BKS modeling was carried out in Solidworks and imported into ANSYS Workbench, as shown in Figure 1. After importing the Solidworks model into ANSYS, a cortical bone block (workpiece) was constructed, representing the surrounding dental bone.

Based on the geometrical models, finite element meshes were generated. The numerical model was prepared in ANSYS 2020 R2[®]—Workbench 2020 R2. The BKS model and the bone disc were meshed with 3D SOLID elements.

In the presented simulation, the BKS tool was provided with TiAl64V parameters as seen in Table 1, and cortical bone (Table 2) with two distinct parameters to compare bone of density D1 ($1.85 \times 10^{-6} \text{ kg/mm}^3$) and D4 ($0.45 \times 10^{-6} \text{ kg/mm}^3$). First, for bone of density D1, an angular velocity of 300 rpm and a feed rate equal to 0.1 mm/s vertically down into the bone were applied. Second, the steps were applied to bone of density D4. In both cases, a thrust load of 80 N was used with a temperature of 39 °C in the absence of irrigation, as it is intended to be used in ongoing research.

Table 1. BKS Implant properties applied in FEA [21,30].

	Ti6Al4V (Grade 5)
Young’s Modulus, MPa	2.0×10^5
Poisson’s Ratio	0.3
Maximum Yield Stress, MPa	1450
Initial Yield Stress, MPa	850
Density, kg/mm^3	4.51×10^{-6}
Coefficient of Thermal Expansion, $1/^\circ\text{C}$	8.5×10^{-6}

Table 2. Bone properties applied in FEA [21,30].

	Cortical Bone
Poisson’s Ratio	0.3
Maximum Yield Stress, MPa	125
Initial Yield Stress, MPa	10
Coefficient of Thermal Expansion, $1/^\circ\text{C}$	8.9×10^5
Young’s Modulus, MPa (D1)	17,000
Young’s Modulus, MPa (D4)	175.12
Density, kg/mm^3 (D1)	1.85×10^{-6}
Density, kg/mm^3 (D4)	0.45×10^{-6}

In the present study, an electric motor EM-12L with a maximum power of 59 W was selected with angular speeds of between 100 and 40,000 rpm [30]. The relation between the torque (M_t in Nm), the maximum electrical power during drilling (P in W), and the speed of rotation (n in rpm) are determined according to Equation (3).

$$M_t = 9.55 \frac{P}{n} \tag{3}$$

According to this equation, the torque is equal to 187.8 Ncm at a rotational speed of 300 rpm. The FEA results obtained were applied to determine optimal parameters for insertion of the new BKS biomechanical design, as seen in Figure 2, relating them to the mathematical concepts used in tribology to support the proposed hypothesis of the lubricating effect of blood when drilling implants into bone, and the advantages of choosing the drilling parameters based on the geometry and surface of the bone implant.

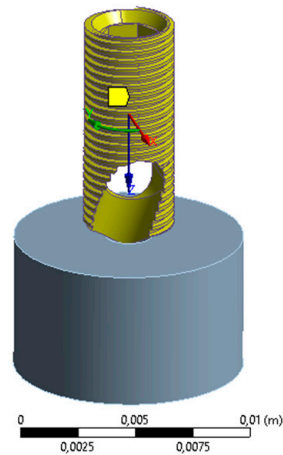


Figure 2. Schematic diagram of BKS Screw in the cortical bone block (workpiece).

3. Results

In previous studies [30] the formation of the plastic strain over different time instants of the bone drilling process was described. As expected, the BKS screw during the drilling process does not present plastic strain. Bone material during perforation presents high plastic strain which increases with the amount of material removed [30–32]. The soft bone (D4) and hard bone (D1) densities used in the thermal-structural analysis show differences in only the equivalent stress values, which, in the case of D1 equals 102.6 MPa, and in the case of D4 equals 1.056 MPa; and normal stress values, which is the case of D1 equals -92.7 MPa, and in the case of D4 equals -0.955 MPa, due to the differences in respective Young moduli. The results for deformation and strain followed the same trend.

3.1. FEA Bone Density D1 (1.85×10^{-6} kg/mm³, 17,000 MPa)

The results of drilling the implant into bone of density D1 are shown in Figures 3–7:

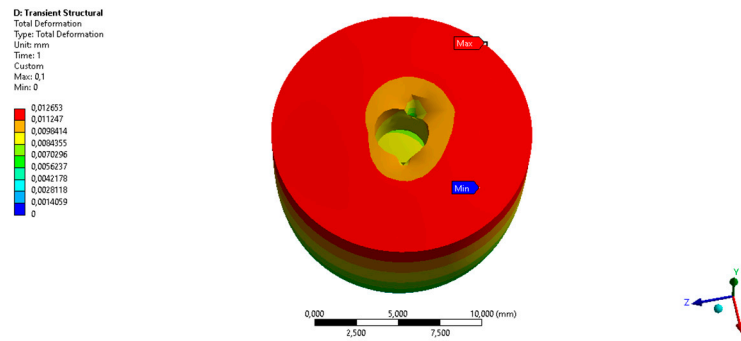


Figure 3. Thermal-Structural Analysis. Bone total deformation 0.013 mm.

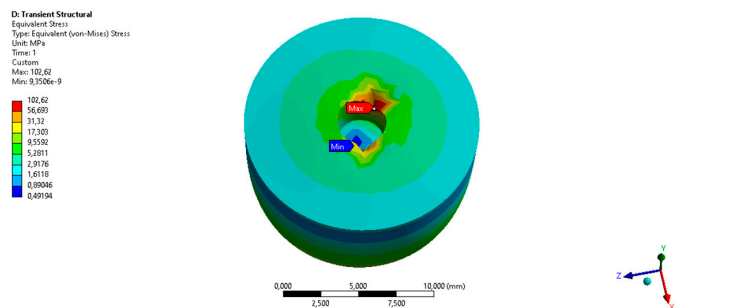


Figure 4. Thermal-Structural Analysis. Equivalent Stress 102.6 MPa.

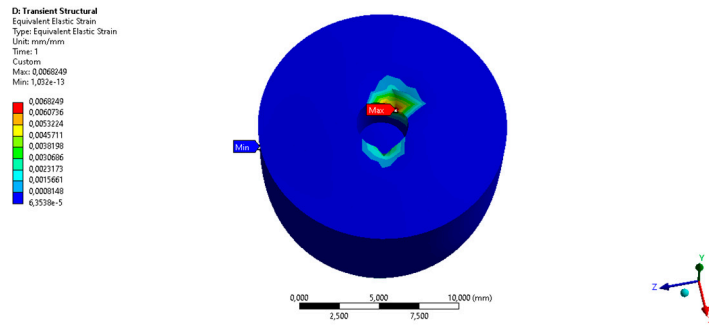


Figure 5. Thermal-Structural Analysis. Equivalent Elastic Strain 0.0068.

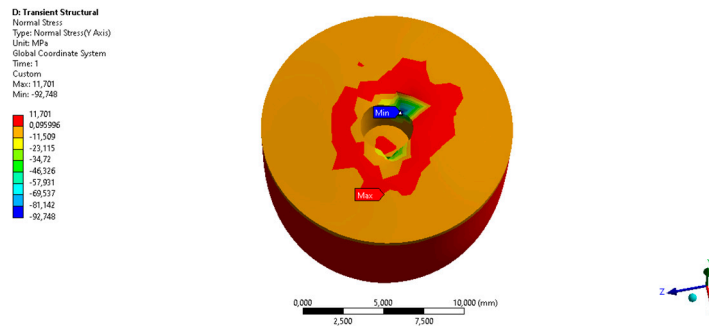


Figure 6. Thermal-Structural Analysis. Y-axis Normal Stress -92.7 MPa.

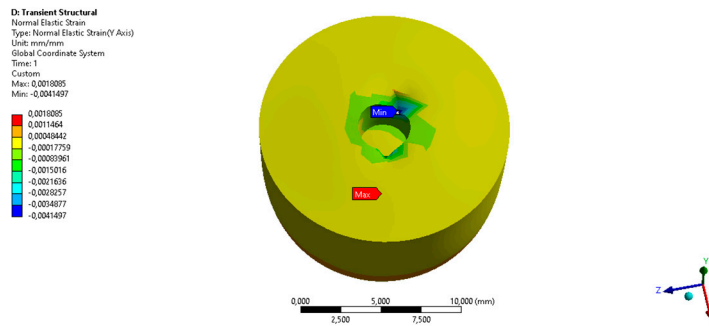


Figure 7. Thermal-Structural Analysis. Y-axis Normal elastic Strain 0.0018.

3.2. FEA Bone Density D4 ($0.45 \times 10^{-6} \text{ kg/mm}^3$, 175.12 MPa)

The results of drilling the implant into bone of density D4 only changed in terms of equivalent and normal stress values, since they depend on the Young modulus.

The displacement and deformation are the same because the remaining conditions are equal, as seen in Figures 8 and 9.

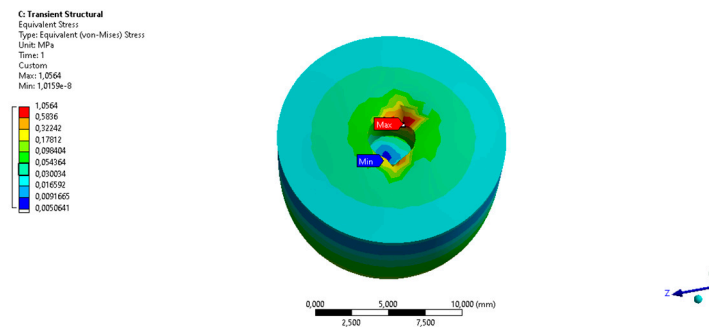


Figure 8. Thermal-Structural Analysis. Equivalent Stress 1.056 MPa.

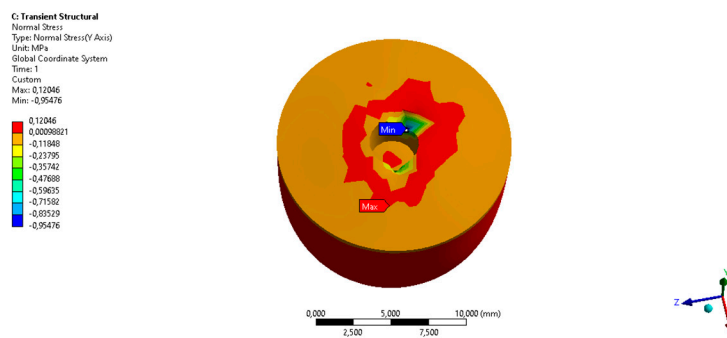


Figure 9. Thermal-Structural Analysis. Y-axis Normal Stress –0.955 MPa.

4. Discussion

Previous studies of BKS implants [22,30–32] obtained by FEA, when analyzed from the biological perspective, describe the plastic deformation promoting bone tissue rupture (osteotomy fracture), blood vessel rupture, the release of salts, enzymes, acids, proteins, macromolecules, and cell death; and the elastic stress/strain of the BKS in the bone, with the blood from cutting and drilling the bone around the screw, and the higher stress/strain obtained in the MIT at the apex of the BKS in contact with the bone at the end of the drilling. As soon as the BKS implant is drilled into the bone, the inflammation process starts through the release of blood adjacent to the cutting, deformation, and stress areas.

Microscopically, the cut bone tissue and blood vessels develop at the interface of the cutting edge of the drilling site, exactly where the bone will be stressed on the threaded walls of the BKS, as analyzed in the results by FEM. Since in the BKS surgical technique, the drilling is not performed by an undersized drill, it is possible to determine and control the plastic and elastic stress/strain, which varies only with the relative bone densities, during the BKS insertion. The coefficient of friction is independent of the applied normal force and the displacement rate [33].

Applying equation (2), where η is the dynamic viscosity of the blood ($4 \times 10^{-3} \text{ N}\cdot\text{s}/\text{m}^2$), N is the entrainment speed of the fluid, that is equal to the velocity of BKS Implant insertion ($5 \times 10^{-4} \text{ m/s}$), and P is the insertion torque applied (1.87 Nm), we can determine the dimensionless lubrication parameter (HN) where, for a given viscosity and load, the Stribeck curve shows how friction changes with increasing velocity, resulting in:

$$HN = \frac{4 \times 10^{-3} \times 5 \times 10^{-4}}{1.87} \tag{4}$$

The lubrication parameter (HN) found within the limitations of the conditions employed in this study is 10.7×10^{-7} for both the cortical bone (D1) and spongy bone (D4) properties defined as shown in Table 2, and the BKS Implant properties in Table 1.

The Stribeck Curve helps us to understand the lubrication regimes where the interface between the bone-implant acts [13]. A meta-analysis [24] compared the suitability of various parameters used to characterize wettability in tribological systems and showed the relationship between wettability and the friction factor for multiple lubricant-surface pairings.

The differences in equivalent stress values, 102.6 MPa, and 1.056 MPa for D1 and D4 respectively, and normal stress values, of –92.7 MPa and –0.955 MPa for D1 and D4, respectively, indicate that the bone blood vessels adjacent to the BIC site suffer different stresses under those densities, which has already been proven in the literature to interfere in the healing process, slowing, or preventing, it [34].

The bleeding and clotting time measures the clotting time of the blood and is dependent on the proper functioning of platelets in the blood vessels with normal hemostasis occurring between 2 and 7 min [35]. Most individuals have a bleeding time of less than 4 min, showing that the lubricating capacity of blood, before its clotting, should become active immediately after cutting the bone through the initial drilling.

More time spent with multiple bone drilling not only damages the bone bed [36] but also increases the time between initial bone drilling and final implant screwing, decreasing the benefit of blood as a lubricant and its sliding across the implant surface [34–36]. With the new BKS design, simultaneous drilling and screwing and low applied speed ensure that the blood acts as a lubricant and can maintain its normal functions. The benefits of blood in intimate contact with the bone-implant surface have already been robustly described in the literature, and the optimal surface for this to occur in a controlled manner is still being sought [18,34].

Bone is tensioned and compressed during the drilling and screwing of implants. On the compression side, bone undergoes a cascade of events that result in upregulated osteoclasts absorbing bone, and, on the tension side, bone undergoes a separate cascade of events that result in upregulated osteoblasts, which create bone. These result in resorption on the compression side and apposition on the tension side, remodeling in such a way that enables the implant to develop long-term osseointegration [37]. By understanding and respecting these parameters, we optimize the probability of achieving controlled and successful results.

Within seconds of the drilling and cutting forces being applied, the bone blood vessels are distorted on the compression side, and they will be partially compressed and partially dilated on the tension side. In minutes, with those blood vessels having been distorted, the blood flow is altered, and oxygen and carbon dioxide levels will change. This change in oxygen tension will trigger inflammatory mediators like prostaglandins and RANKL to be released [38].

Limitations in experimental in vivo research and computational modeling due to the not-well-established mixed-lubrication mechanism, the high computational costs required to model the bearing surfaces within a relatively large contact area, and the complexity of geometry analyzing lubrication of biological and non-biological surfaces (drilling bone screws, hip, and knee joints) with biological lubricants, inhibit the development of the field of tribology [27,39].

Highlighting the importance of the inflammatory process and the lubricating effect of the blood during bone drilling, we can promote future studies to determine other blood lubrication parameters at different bone densities, different blood viscosities (pathologies), other bone screw insertion speeds, and different implant geometries, comparing the results and improving the osseointegration prognosis. In addition, biofunctionalization may shorten the healing period of osseointegrated biomaterials [40].

5. Conclusions

A new BKS biomechanism for bone screws and implants was presented as a bone implant screw to show how blood could influence the resulting friction between bone-implant surfaces, correlating with mechanical and biological properties, defining a novel approach to obtain a new lubricant parameter in the analysis of drilling into bone. The natural effect of blood as a lubricant in bone-screw perforations is not investigated in the literature and its effects are paramount in bone healing. This work has elucidated the relevance of blood as a lubricant in drilling and screwing bone at lower speeds with pre-defined parameters.

The lubrication parameter (HN) found within the limitations of the conditions employed in this study is 10.7×10^{-7} for both cortical bone (D1) and spongy bone (D4).

Thermal-structural analysis of soft bone (D4) and hard bone (D1) densities shows differences only in equivalent stress values, due to the differences in respective Young moduli. This is ongoing research and future studies will be able to experimentally determine the advantages and disadvantages of blood as a bio-lubricant.

Author Contributions: Conceptualization, C.A.A.; methodology, C.A.A.; formal analysis, C.A.A.; investigation, C.A.A.; writing—original draft preparation, C.A.A.; writing—review and editing, E.M.M.F.; visualization, E.M.M.F.; supervision, R.N.J. All authors have read and agreed to the published version of the manuscript.

Funding: This research received no external funding.

Data Availability Statement: Not applicable.

Conflicts of Interest: The authors declare no conflict of interest.

References

1. Vahedi, A.; Bigdelou, P.; Farnoud, A.M. Quantitative analysis of red blood cell membrane phospholipids and modulation of cell-macrophage interactions using cyclodextrins. *Sci. Rep.* **2020**, *10*, 15111. [[CrossRef](#)] [[PubMed](#)]
2. Minton, K. Red blood cells join the ranks as immune sentinels. *Nat. Rev. Immunol.* **2021**, *21*, 760–761. [[CrossRef](#)] [[PubMed](#)]
3. Mathew, J.; Sankar, P.; Varacallo, M. Physiology, Blood Plasma. In *StatPearls*; StatPearls Publishing: Treasure Island, FL, USA, 2022.
4. Generalov, V.M.; Safatov, A.S.; Kruchinina, M.V. Dielectric Properties of the Human Red Blood Cell. *Meas. Tech.* **2020**, *63*, 580–586. [[CrossRef](#)]
5. Ahmed, M.H.; Ghatge, M.S.; Safo, M.K. Hemoglobin: Structure, Function and Allostery. *Subcell. Biochem.* **2020**, *94*, 345–382. [[CrossRef](#)]
6. Tutwiler, V.; Singh, J.; Litvinov, R.I.; Bassani, J.L.; Purohit, P.K.; Weisel, J.W. Rupture of blood clots: Mechanics and pathophysiology. *Sci. Adv.* **2020**, *6*, eabc0496. [[CrossRef](#)] [[PubMed](#)]
7. Li, J.; Sapkota, A.; Kikuchi, D.; Sakota, D.; Maruyama, O.; Takei, M. Red blood cells aggregability measurement of coagulating blood in extracorporeal circulation system with multiple-frequency electrical impedance spectroscopy. *Biosens. Bioelectron.* **2018**, *112*, 79–85. [[CrossRef](#)]
8. Stauffer, E.; Loyrion, E.; Hanco, I. Blood viscosity and its determinants in the highest city in the world. *J. Physiol.* **2020**, *598*, 4121–4130. [[CrossRef](#)]
9. Makowiecki, A.; Hadzik, J.; Błaszczyzyn, A.; Gedrange, T.; Dominiak, M. An evaluation of superhydrophilic surfaces of dental implants—a systematic review and meta-analysis. *BMC Oral Health* **2019**, *19*, 79. [[CrossRef](#)]
10. Florencio-Silva, R.; Sasso, G.R.; Sasso-Cerri, E.; Simões, M.J.; Cerri, P.S. Biology of Bone Tissue: Structure, Function, and Factors That Influence Bone Cells. *Biomed Res. Int.* **2015**, *2015*, 421746. [[CrossRef](#)]
11. Raj, A.; Rajak, D.K.; Gautam, S.; Guria, C.; Pathak, A.K. Shear Rate Estimation: A Detailed Review. In Proceedings of the Paper Presented at the Offshore Technology Conference, Houston, TX, USA, 2–5 May 2016. [[CrossRef](#)]
12. Gu, C.; Meng, X.; Xie, Y.; Zhang, D. The influence of surface texturing on the transition of the lubrication regimes between a piston ring and a cylinder liner. *Int. J. Eng. Res.* **2017**, *18*, 785–796. [[CrossRef](#)]
13. Veltkamp, B.; Velikov, K.P.; Venner, C.H.; Bonn, D. Lubricated Friction and the Hersey Number. *Phys. Rev. Lett.* **2021**, *126*, 044301. [[CrossRef](#)] [[PubMed](#)]
14. Straumal, B.B.; Gornakova, A.S.; Kiselevskiy, M.V. Optimal surface roughness of Ti6Al4V alloy for the adhesion of cells with osteogenic potential. *J. Mater. Res.* **2022**, *37*, 2661–2674. [[CrossRef](#)]
15. Kamynina, O.K.; Kravchuk, K.S.; Lazov, M.A. Effect of Surface Roughness on the Properties of Titanium Materials for Bone Implants. *Russ. J. Inorg. Chem.* **2021**, *66*, 1073–1078. [[CrossRef](#)]
16. Boyan, B.D.; Lotz, E.M.; Schwartz, Z. Roughness and Hydrophilicity as Osteogenic Biomimetic Surface Properties. *Tissue Eng. Part A* **2017**, *23*, 1479–1489. [[CrossRef](#)] [[PubMed](#)]
17. Wang, C.; Zhang, G.; Li, Z.; Zeng, X.; Xu, Y.; Zhao, S.; Hu, H.; Zhang, Y.; Ren, T. Tribological behavior of Ti-6Al-4V against cortical bone in different biolubricants. *J. Mech. Behav. Biomed. Mater.* **2019**, *90*, 460–471. [[CrossRef](#)]
18. Lian, Z.; Guan, H.; Ivanovski, S.; Loo, Y.C.; Johnson, N.W.; Zhang, H. Effect of bone to implant contact percentage on bone remodeling surrounding a dental implant. *Int. J. Oral Maxillofac. Surg.* **2010**, *39*, 690–698. [[CrossRef](#)] [[PubMed](#)]
19. Lee, J.W.Y.; Bance, M.L. Physiology of Osseointegration. *Otolaryngol. Clin. N. Am.* **2019**, *52*, 231–242. [[CrossRef](#)]
20. Rahmanpanah, H.; Mouloudi, S.; Burvill, C.; Gohari, S.; Davies, H.M.S. Prediction of load-displacement curve in a complex structure using artificial neural networks: A study on a long bone. *Int. J. Eng. Sci.* **2020**, *154*, 103319. [[CrossRef](#)]
21. Maria, G.F.; Elza, M.F.; Renato, M.N. Three-dimensional dynamic finite element and experimental models for drilling processes. *Proc. IMechE. Part L J. Mater. Des. Appl.* **2015**, *232*, 35–43.
22. Andreucci, C.A.; Fonseca, E.M.M.; Jorge, R.N. Increased Material Density within a New Biomechanism. *Math. Comput. Appl.* **2022**, *27*, 90. [[CrossRef](#)]
23. Wang, S.-H.; Shen, Y.-W.; Fuh, L.-J.; Peng, S.-L.; Tsai, M.-T.; Huang, H.-L.; Hsu, J.-T. Relationship between Cortical Bone Thickness and Cancellous Bone Density at Dental Implant Sites in the Jawbone. *Diagnostics* **2020**, *10*, 710. [[CrossRef](#)] [[PubMed](#)]
24. Schertzer, M.J.; Iglesias, P. Meta-Analysis Comparing Wettability Parameters and the Effect of Wettability on Friction Coefficient in Lubrication. *Lubricants* **2018**, *6*, 70. [[CrossRef](#)]

25. Shacham, S.; Castel, D.; Gefen, A. Measurements of the static friction coefficient between bone and muscle tissues. *J. Biomech. Eng.* **2010**, *132*, 084502. [[CrossRef](#)] [[PubMed](#)]
26. Dannaway, J.; Dabirrahmani, D. An investigation into the frictional properties between bone and various orthopedic implant surfaces—implant stability. *J. Musculoskelet.* **2015**, *18*, 1550015. [[CrossRef](#)]
27. Haoyu, Z.; Zhang, X.; Jun, S.; Dagang, W. A study of misaligned compliant journal bearings lubricated by non-Newtonian fluid considering surface roughness. *Trib. Int.* **2023**, *179*, 108138. [[CrossRef](#)]
28. Halldin, A.; Jinno, Y.; Galli, S.; Ander, M.; Jacobsson, M.; Jimbo, R. Implant stability and bone remodeling up to 84 days of implantation with an initial static strain. An in vivo and theoretical investigation. *Clin. Oral Impl. Res.* **2016**, *27*, 1310–1316. [[CrossRef](#)] [[PubMed](#)]
29. Makary, C.; Rebaudi, A.; Mokbel, N.; Naaman, N. Peak Insertion Torque Correlated to Histologically and Clinically Evaluated Bone Density. *Impl. Dent.* **2011**, *20*, 182–191. [[CrossRef](#)] [[PubMed](#)]
30. Andreucci, C.A.; Fonseca, E.M.M.; Natal, R.M.J. Structural analysis of the new Bioactive Kinetic Screw in titanium alloy vs. commercially pure titanium. *J. Comp. Art. Int. Mec. Biomec.* **2022**, *2*, 35–43. [[CrossRef](#)]
31. Andreucci, C.A.; Alshaya, A.; Fonseca, E.M.M.; Jorge, R.N. Proposal for a New Bioactive Kinetic Screw in an Implant, Using a Numerical Model. *Appl. Sci.* **2022**, *12*, 779. [[CrossRef](#)]
32. Andreucci, C.A.; Fonseca, E.M.M.; Jorge, R.N. 3D Printing as an Efficient Way to Prototype and Develop Dental Implants. *BioMedInformatics* **2022**, *2*, 44. [[CrossRef](#)]
33. Trzepiecinski, T. A Study of the Coefficient of Friction in Steel Sheets Forming. *Metals* **2019**, *9*, 988. [[CrossRef](#)]
34. Xing, G.; Manon, F.; Guillaume, H. Biomechanical behaviours of the bone–implant interface: A review. *J. R. Soc. Interface* **2019**, *16*, 20190259. [[CrossRef](#)]
35. Milillo, L.; Cinone, F.; Lo Presti, F.; Lauritano, D.; Petruzzi, M. The Role of Blood Clot in Guided Bone Regeneration: Biological Considerations and Clinical Applications with Titanium Foil. *Materials* **2021**, *14*, 6642. [[CrossRef](#)] [[PubMed](#)]
36. Tsiagadigui, J.G.; Ndiwe, B.; Yamben, M.N.; Fotio, N.; Belinga, F.E.; Njeugna, E. The effects of multiple drilling of a bone with the same drill bit: Thermal and force analysis. *Heliyon* **2022**, *8*, e08927. [[CrossRef](#)]
37. Pallua, J.D.; Putzer, D.; Jäger, E.; Degenhart, G.; Arora, R.; Schmölz, W. Characterizing the Mechanical Behavior of Bone and Bone Surrogates in Compression Using pQCT. *Materials* **2022**, *15*, 5065. [[CrossRef](#)] [[PubMed](#)]
38. Anesi, A.; Cavani, F. Editorial for the Special Issue on “Multidisciplinary Insights on Bone Healing”. *Biology* **2022**, *11*, 1776. [[CrossRef](#)]
39. Anitua, E. Biological drilling: Implant site preparation in a conservative manner and obtaining autogenous bone grafts. *Balk. J. Dent. Med.* **2018**, *22*, 98–101. [[CrossRef](#)]
40. Cirera, A.; Manzanares, M.C.; Sevilla, P.; Ortiz-Hernandez, M.; Galindo-Moreno, P.; Gil, J. Biofunctionalization with a TGFβ-1 Inhibitor Peptide in the Osseointegration of Synthetic Bone Grafts: An In Vivo Study in Beagle Dogs. *Materials* **2019**, *12*, 3168. [[CrossRef](#)]

Disclaimer/Publisher’s Note: The statements, opinions and data contained in all publications are solely those of the individual author(s) and contributor(s) and not of MDPI and/or the editor(s). MDPI and/or the editor(s) disclaim responsibility for any injury to people or property resulting from any ideas, methods, instructions or products referred to in the content.